



# JOURNAL OF NATURAL RESOURCES AND DEVELOPMENT

## Research article

# *Using global data products to improve the understanding of eco-hydrological processes and patterns in tropical catchments*

Saúl Arciniega-Esparza<sup>1</sup>, Christian Birkel<sup>2,3</sup>

<sup>1</sup> Hydrogeology Group, Faculty of Engineering, National Autonomous University of Mexico, Mexico City, Mexico; [sarciniegae@comunidad.unam.mx](mailto:sarciniegae@comunidad.unam.mx)

<sup>2</sup> Department of Geography and Water and Global Change Observatory, University of Costa Rica, San José, Costa Rica;

<sup>3</sup> Leibniz Institute for Freshwater Ecology and Inland Fisheries, Berlin, Germany; [CHRISTIAN.BIRKEL@ucr.ac.cr](mailto:CHRISTIAN.BIRKEL@ucr.ac.cr)

## Article history

Received 18.10.2024  
Accepted 12.11.2024  
Published 27.03.2025

## Keywords

Tropics  
Eco-hydrology  
Water use efficiency  
Budyko  
Latin America

## Abstract

Understanding large-scale eco-hydrological processes in tropical regions across Latin America has been a challenge due to climate variability and the lack of long temporal data series. As an alternative, remote sensing data and global products have been widely used in ungauged basins to get insights into key hydro-climatic patterns. Here, we study eco-hydrological processes in 27 tropical catchments across Colombia, Costa Rica and Mexico through the vegetation water use efficiency described by the Horton Index (HI) and the long-term water-energy balance described by the Budyko curve. Streamflow records from 2000 to 2014 were correlated with vegetation and climate indexes derived from MODIS, TRMM and CHIRPS at long-term and annual scales in order to find which factors presented more influence on the catchment's response. Most of the Colombian and Costa Rican catchments were classified as energy-limited according to the dryness index ( $AI > 1$ ) and low water efficiency ( $HI \sim 0.48$ ), meanwhile, Mexican catchments tended to be water-limited ( $AI > 1$ ) and more water efficient ( $HI \sim 0.52$ ). Results suggested that climate is the strongest driver of water partitioning, where mean annual precipitation presented a strong linear relationship ( $\rho = 0.93$ ) with mean annual and intra-annual streamflow. Furthermore, the dryness index was a good predictor ( $r^2 = 0.83$  and  $0.86$ , respectively) of the annual and long-term streamflow through a non-linear relationship similar to Budyko theory. Vegetation water use efficiency plays a secondary role in water partitioning, where HI was linearly negatively correlated with streamflow and baseflow ( $\rho = -0.78$  and  $0.82$ ).

## 1. Introduction

Eco-hydrology examines interactions between the structure and function of ecological systems and hydrological processes, including water partitioning, storage, and freshwater connectivity (Guswa et al., 2020), which are critical concerns for water security in the face of anthropogenic alterations and future climate change. This is especially important in tropical climates, where eco-hydrological processes differ compared to extra-tropical regions, mainly due to higher rates of precipitation  $P$  than potential evapotranspiration  $PET$  (Moore et al., 2015; Koppa et al., 2021; Zomer et al., 2022). The often-resulting high runoff  $R$  with respect to the catchment area is affected by the inter-annual variation of the Inter-tropical Convergence Zone (ITZC), that leads to more days per year of thunderstorms and tropical cyclones (Syvitski et al., 2014). Tropical land areas only cover 19% of the total land surface (Peel et al., 2007) and tropical forests ~50% of tropical climates. Nevertheless, these forests represent an important storage of terrestrial biomass and carbon (~17-25%) and globally the highest annual net primary productivity ANPP (~22-35%) (Prentice et al., 2001).

For comparison purposes of large-scale eco-hydrological processes, identifying similar drivers of catchment functioning proved to be a fruitful endeavor (Wagener et al., 2007; Chen et al., 2023). Long-term climate has been identified as the first order driver for water availability and ecosystem conditions, controlling many functions at the catchment scale (Sawicz et al., 2011; Zhang et al., 2017).

Catchment characteristics are further second order drivers, as topography, geology and land cover (Peña-Arancibia et al., 2010; Sawicz et al., 2011; Birkel et al., 2012; Beck et al., 2015; Gnann et al., 2025). Indeed, vegetation plays an important role in tropical water budgets, where forested areas show a negative correlation with runoff generation at the annual scale (Bruijnzeel, 2004; Zhang et al., 2017; Xiong et al., 2023). The latter is particularly important in the seasonally dry tropics where forest cover was reported to sustain higher dry season streamflow (Krishnaswamy et al., 2018). In comparison with other climates, tropical vegetation evolved to capture nutrients and light more efficiently than water (Nemani et al., 2003; Yang et al., 2015), leading to a mostly unchanged hydrological partitioning under increased CO<sub>2</sub> emission scenarios (Yang et al., 2016). At the same time, water availability in tropical catchments is correlated with vegetation root depth, where deeper roots are linked to large evapotranspiration rates (Gan et al., 2021).

This co-evolution between biophysical factors, geological properties and climate drivers controls the annual hydrological behavior of catchments (Brooks et al., 2011; Troch et al., 2009; Voepel et al., 2011). Budyko's (1974) framework links the long-term water and energy balances through a relationship between evapotranspiration (related to vegetation), precipitation and net radiation and its relationship to runoff generation mechanisms (Trancoso et al., 2016). The Budyko's theory represents a tool to evaluate the water balance sensitivity to changes in climate and land use at catchment-scales (Thompson et al., 2011; Peña-Arancibia et al., 2012; Esquivel-Hernández et al., 2017; Gan et al., 2021; Collignan et al., 2023).

In more detail, inter-annual hydrological partitioning can be assessed using the Horton Index HI similar to Troch et al. (2009) based on work by Horton (1933) and Huxman et al. (2004). The latter authors showed how vegetation biomes are adapted to a common maximum water use efficiency ( $WUE=ANPP/P$ ) under drought conditions. The HI tends to be constant from year to year despite inter-annual precipitation seasonality. The HI is derived as the ratio between vaporization (evapotranspiration) and wetting of a catchment-scale and was related with catchment mean slope and elevation (Voepel et al., 2011), and more recently to deep storage dynamics in dry environments (Arciniega-Esparza et al., 2017).

However, eco-hydrological partitioning approaches are data dependent, and tropical catchments have been poorly studied mostly due to the scarce climate and streamflow monitoring compared to e.g. temperate regions (Esquivel-Hernández et al., 2017; Montanari et al., 2006). Hence remote sensing data and global products are needed to better understand spatial and temporal hydrological patterns across tropical regions such as, for example, climatic effects on riverine fluxes (Syvitski et al., 2014), droughts and water availability (Muñoz-Jiménez et al., 2018), patterns of groundwater storage and discharge (Peña-Arancibia et al., 2010a) and the influence of groundwater on the Amazon water cycle (Pokhrel et al., 2013).

Critical issues in using gridded precipitation products remain, as remotely sensed data require ground-truthing with local station observations (Zambrano-Bigiarini et al., 2017). Nevertheless, using remote sensing data and global products together with station observations of precipitation and streamflow can advance our knowledge of poorly understood eco-hydrological processes with limited data in tropical catchments. Our objectives therefore are to

- a) understand large-scale vegetation water use efficiency across tropical biomes of Latin America and
- b) analyze spatio-temporal patterns of water use efficiency using the Budyko theory and the Horton Index in 27 catchments across Central America and South America.

Results obtained are of interest to understand the impacts of climate and vegetation changes on water availability in tropical catchments under future scenarios.

---

## 2. Data and Methods

### 2.1 Study region

The study area comprises 27 catchments with daily streamflow records between 1980-2003, some more recent until 2010 across the Latin American tropics. The catchments are located between 3.0° to 19.5°N and 72° to 100°W from Mexico, Costa Rica to Colombia (8, 10 and 9 catchments, respectively), as shown in Figure 1 A. The study area exhibits tropical climates (Peel et al., 2007) and is covered mainly by evergreen broadleaf forest and savanna trees (Figure 1 B).

A topographical barrier is formed by the “Pacific ring of fire” as tectonic plates divide the catchments into the Pacific Ocean and the Caribbean Sea continental basins. The Pacific catchments exhibit a more pronounced precipitation seasonality shown as dark blue regions in Figure 1 C, meanwhile; Caribbean catchments show a more uniform monthly precipitation distribution.

Table 1 shows the topography and geomorphological catchment properties that were derived from the Shuttle Radar Topography Mission (STRM) at 90 m resolution (Farr et al., 2007) using SAGA GIS terrain analysis tools (Conrad et al., 2015). The total catchment area covers ~98,000 km<sup>2</sup> and spans an elevation range from 200 to 2,500 m.a.s.l., with a median of 1,100 m.a.s.l. Catchments' slopes vary from 1.3 to 19.2 degrees and a preferred south-facing aspect (~180 degrees). The topographic wetness index (TWI) varies from 7.2 to 9.7, where Colombian catchments tend to be topographically wetter than others. Catchments' climatology and vegetation properties are described in the following sections.

---

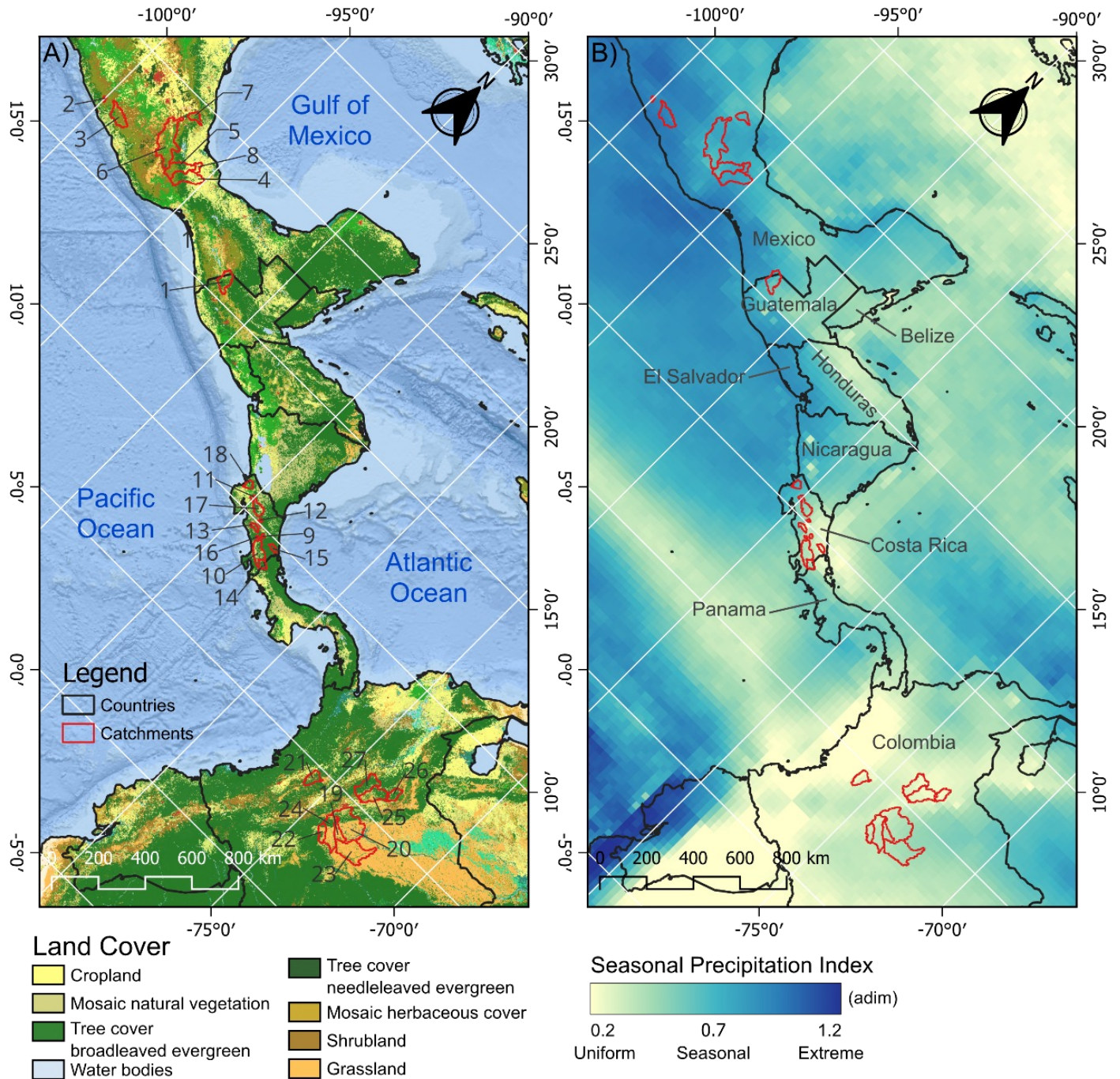


**Figure 1:** A) Spatial distribution of the 27 analyzed catchments and land cover derived from MODIS, B) the seasonal precipitation index that explains the monthly distribution of precipitation.

**Table 1:** Physiographic properties of catchments used in this study with assigned ID, Kc is the Gravelius shape index, TWI is the topographic wetness index. Climate classification used the Köppen-Geiger system.

Country	ID	Name	Climate class*	Area [km <sup>2</sup> ]	Perimeter [km]	Kc	Elevation [masl]	Slope [deg]	Aspect [deg]	TWI
	1	30158	Cfb-Cwb	3663.13	464.58	2.17	1710.46	13.53	190.4	7.87
	2	20022	Aw	225.32	90.72	1.7	1829.32	18.06	159.97	7.23
	3	20037	Aw	3978.49	524.7	2.35	1312.16	16.72	179.72	7.38
	4	28001	Am	5684.33	612	2.29	480.15	8.83	168.45	8.27
Mexico	5	28013	Am-Cwb	4592.98	601.38	2.5	981.7	14.12	173.62	7.76
	6	28015	Cfb-Cwb	11981.76	1097.82	2.83	1868.63	14.07	176.36	7.82
	7	28125	Aw-Cfb	1525.55	262.26	1.89	1731.4	12.06	141.12	7.91
	8	28136	Am	5612.1	744.12	2.8	814.34	11.77	176.66	8.1
	9	Oriente	Cfb	229.17	71.14	1.33	1415.78	17	169.46	7.52
	10	Palmar	Am	4771.38	412.89	1.69	1069.38	12.58	185.86	8.06
	11	Rancho Rey	Am	320.27	102.81	1.62	495.05	6.47	223.09	8.61
	12	Tacares	Af	200.62	73.11	1.46	1414.54	7.36	211.89	8.64
Costa Rica	13	El Rey	Am	656.48	149.21	1.64	1144.47	15.94	189.59	7.6
	14	Caracucho	Af	1133.29	184.67	1.55	1253.98	10.33	204.53	8.14
	15	Pandora	Af	637.35	133.49	1.49	599.16	13.34	156.58	7.94
	16	Providencia	Cfb	122.15	54.02	1.38	2575.82	19.22	196.7	7.41
	17	Terron Colorado	Am	2061.27	259.2	1.61	737.51	8.72	175.99	8.62
	18	Guardia	Am	960.67	154.73	1.41	340.41	4.47	200.51	9.33
	19	35017040	Am	2352.44	431.64	2.51	469.05	3.18	144.5	9.68
	20	35107030	Am	14541.48	882.72	2.06	958.03	7.3	155.82	9.26
	21	26127040	Af-Cfb	2826.45	367.56	1.95	1796.81	12.13	213.09	8.08
	22	32077070	Am	2152.14	353.34	2.15	771.25	9.02	156.73	8.58
Colombia	23	35127010	Am	9846.17	853.38	2.43	205.98	1.29	172.4	9.44
	24	32077080	Am	5866.69	669.6	2.47	1102.9	8.93	159.13	8.98
	25	24017570	Cfb	5374.88	567.9	2.19	2490.5	10.3	190.28	8.4
	26	24027010	Af	2098.85	319.68	1.97	2251.68	16.67	195.84	7.77
	27	23127060	Af	4954.62	560.7	2.25	1295.82	14.19	201.22	7.86

## 2.2 Data

The time series of daily streamflow were obtained from different sources, shown in Table 2. The study period was established from 2000 to 2015; only near-natural streamflow regimes were selected, and a minimum period of three years (after 2000) was needed to overlap with the period of some remote sensing datasets (as described below). Years of streamflow records were ignored when more than 10% of missing data was found.

**Table 2:** Streamflow records and sources.

ID	Country	Institution	Source	Station Name	Start date	End date
1	Mexico	National Water Commission (CONAGUA)	Surface water database (BANDAS) available at <a href="https://app.conagua.gob.mx/bandas/">https://app.conagua.gob.mx/bandas/</a>	30158	1980-01	2008-12
2				20022	1980-01	2003-10
3				20037	1980-01	2007-12
4				28001	1982-01	2011-12
5				28013	1980-01	2011-12
6				28015	1982-01	2011-12
7				28125	1980-01	2011-12
8				28136	1982-01	2011-12
9	Costa Rica	Costa Rican Electricity Institute (ICE)		Oriente	1990-01	2003-12
10				Palmar	1990-01	2003-12
11				Rancho Rey	1990-01	2003-12
12				Tacares	1990-01	2003-12
13				El Rey	1990-01	2003-12
14				Caracucho	1990-01	2003-12
15				Pandora	1990-01	2003-12
16				Providencia	1990-01	2003-12
17				Terron Colorado	1990-01	2003-12
18				Guardia	1990-01	2003-12
19	Colombia	Institute of Hydrology Meteorology and Environmental Studies (IDEAM)	Consultation and Download of Hydrometeorological Data <a href="http://dhime.ideam.gov.co/atencionciudadano/">http://dhime.ideam.gov.co/atencionciudadano/</a>	35017040	1983-01	2011-12
20				35107030	1986-03	2015-12
21				26127040	1980-01	2015-12
22				32077070	1986-01	2015-12
23				35127010	1980-01	2010-12
24				32077080	1980-01	2017-12
25				24017570	1980-01	2014-12
26				24027010	1984-01	2014-12
27				23127060	1980-01	2005-12

The catchments' eco-hydrological conditions were derived from four datasets and detailed information of the datasets is given in Table 3. Precipitation (P) was obtained from two global products: the Climate Hazards Group InfraRed Precipitation with Satellite data (CHIRPS version 2, Funk et al., 2015), a global daily precipitation product that combines remote sensed precipitation from five different satellite products and includes a calibration procedure using more than 200 ground stations; and the Tropical Rainfall Measuring Mission (TRMM product 3B43), a global monthly precipitation product that was created using TRMM-adjusted merged microwave-infrared precipitation rate and corrections with rain gauges. Evapotranspiration and potential evapotranspiration were obtained from the Moderate Resolution Imaging Spectroradiometer (MODIS 16A3), distributed by the Numerical Terradynamic Simulation Group at the University of Montana and comprises a global yearly and monthly dataset of evapotranspiration/latent heat flux product based on the Penman-Monteith equation, which includes inputs of other MODIS products (Mu et al., 2011). Finally, vegetation indexes were obtained from MODIS13Q1 (Didan, 2015), a global 16-day product that incorporates an 8-day composite of surface reflectance granules and derives the Normalized Vegetation Index (NDVI) and the Enhanced Vegetation Index (EVI).

For the purposes of this study, CHIRPS was used as the main precipitation source for catchment-scale analysis due to the higher spatial resolution in comparison to TRMM and because it showed a good performance across Central America and South American regions (Muñoz-Jiménez et al., 2018; Zambrano-Bigiarini et al., 2017). Whereas, the TRMM dataset was used in combination with MODIS to derive maps that describe the spatial variation of climatic indices across the study area.

For the catchment scale analysis, the study period covers from 2000 to the most recent period for each streamflow gauge (2003 to 2010), and from 2000 to 2014 for the spatial analysis using climatological indices.

**Table 3:** Remote sensing data source and brief description of each global product used.

Dataset	Variable	Label	Resolution	Period	Scale	Data type	Source
CHIRPSv2.0	Precipitation	P	0.05°	1981-present	daily	Merged remote sensing interpolated and calibrated	Funk et al. (2015)
TRMM3B43	Precipitation	P	0.25°	1998-present	monthly	Remote sensing calibrated	Bolvin and Huffman (2015)
MODIS16A3	Evapotranspiration, Potential Evapotranspiration	ET, PET	500m	2000-2014	monthly	Remote sensing	Mu et al. (2011)
MODIS13Q1	Vegetation Indices	NDVI, EVI	250m	2000-present	16 days	Remote sensing	Didan (2015)

## 2.3 Methods

We computed different metrics to characterize the long-term eco-hydrological behavior of catchments. Such indicators include the mean annual precipitation  $P$ , evapotranspiration  $AET$ , potential evapotranspiration  $PET$ , streamflow  $Q$  and vegetation indexes (NDVI and EVI). The Budyko framework (Budyko, 1974) was implemented to relate the long-term water and energy balances, where  $AET$  can be derived from  $P$  and  $PET$  as follows:

$$EI = \sqrt{AI * \tanh(AI^{-1}) * (1 - \exp(-AI))}, \quad (1)$$

where  $EI$  is the evaporative index ( $AET/P$ ) and  $AI$  is the dryness index ( $PET/P$ ). Eq. 1 assumes that  $AET$  is limited by water availability and energy, thus, the catchment eco-hydrological behavior can be affected by climate change ( $P$  or  $PET$ ) or modifications of land use and vegetation ( $AET$ ).

The Horton index  $HI$  proposed by Troch et al. (2009) was chosen as the ecosystems' rainwater use efficiency indicator, which is computed as the vaporization-to-wetting ratio:

$$HI = \frac{V}{W} = \frac{P-Q}{P-Qd}, \quad (2)$$

where  $V$  is the annual vaporization,  $W$  is the wetting derived from the portion of precipitation retained by the catchment at storm time scales,  $P$  is the annual precipitation,  $Q$  is the annual streamflow,  $Qd$  is the annual runoff.

The  $HI$  was computed annually, and the mean value was estimated in order to find long-term controls on water use efficiency. On the other hand, at annual scales, if  $V$  is comparable to  $AET$ , then we can rewrite Eq. 2 as:

$$EHI = \frac{V}{W} = \frac{AET}{P-Qd}, \quad (3)$$

Equations 1 and 2 were compared using different global products and in-situ data to evaluate the impact of data sources on catchments' eco-hydrological behavior.

Daily streamflow  $Q_t$  was separated into baseflow  $Q_{bt}$  and direct runoff  $Q_{dt}$  using the one parameter recursive filter (Lyne and Hollick, 1979):

$$Q_{dt} = \alpha Q_{dt-1} + \frac{1+\alpha}{2}(Q_t - Q_{t-1}), \quad (4)$$

$$Q_{bt} = Q_t - Q_{dt}, \quad (5)$$

where  $0 \leq Q_{dt} \leq Q_t$  and  $\alpha$  is a filter parameter that ranges between 0.9-0.95. For this analysis,  $\alpha$  was set to 0.9. This filter is applied three times (forward, backward and forward in time) to obtain a smoothed signal of  $Q_b$ .

In order to compute an indicator of the contribution of groundwater to river flow at catchment-scales, we used the baseflow index BFI as the ratio between the annual baseflow volume  $Q_b$  and the annual streamflow volume  $Q$  (Smakhtin, 2001):

$$BFI = \frac{Q_b}{Q}, \quad (6)$$

The long-term mean BFI was computed for each catchment.

To evaluate the effect of inter-annual climatology on long-term catchment responses, we calculated the seasonal index proposed by Walsh and Lawler (1981):

$$SI = \frac{1}{X_a} \sum_{m=1}^{12} \left| X_m - \frac{X_a}{12} \right|, \quad (7)$$

where  $X_a$  is the mean annual variable and  $X_m$  is the mean value of month  $m$ . A high SI value means that the climate is seasonal, and a low value indicates a more uniformly distributed climatology throughout the year. The SI was computed for P, AET, PET, Q and  $Q_b$ .

## 3. Results

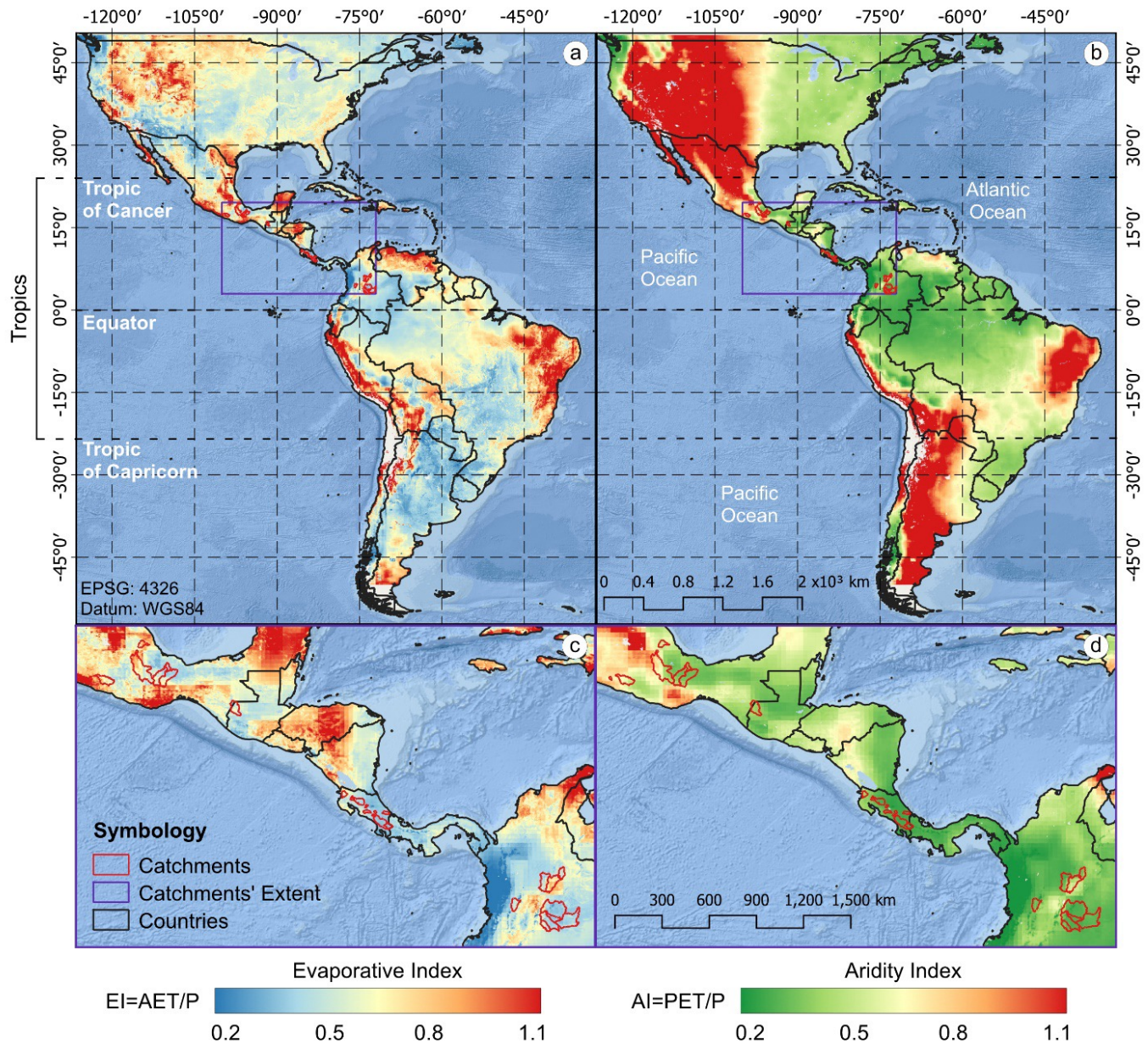
### 3.1 Budyko water-energy balance across tropical climates

The spatial distribution of the long-term Budyko water-energy indexes (EI and AI) for the period 2000-2014 across America (50°S-45°N) are shown in Figure 2. The AI and EI showed spatial similarities between latitude 0-30°S, where high AI and EI values ( $>3$  and  $\geq 11$ , respectively) overlapped in low density forest areas. For latitude 0-30°N, Budyko's indexes did not show a spatial correlation as some arid regions exhibited AI greater than 5 and EI around 0.4, whereas wetter regions presented AI values around 1.5 and EI close to 1.

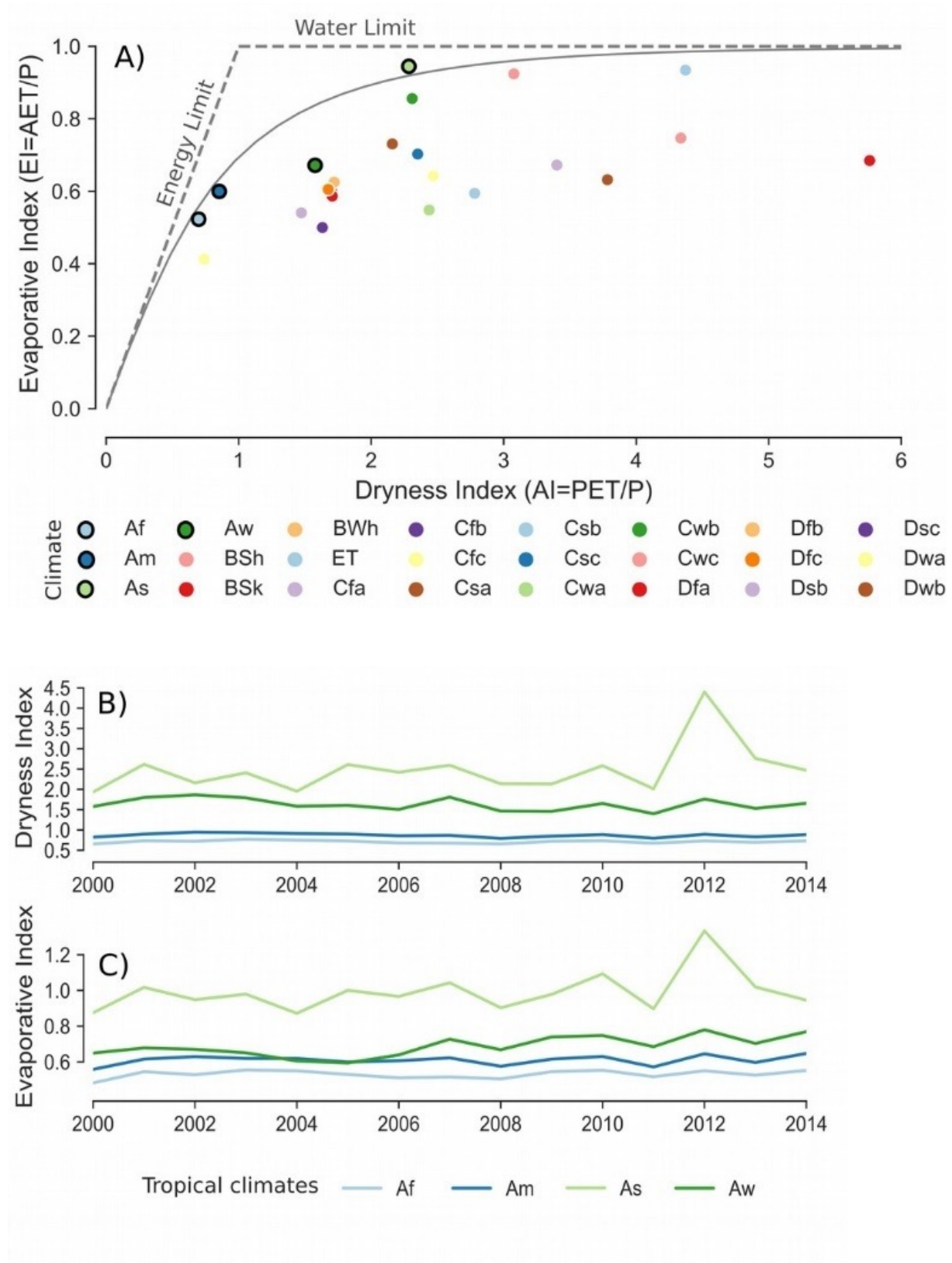
Tropical climates exhibited dryness index values that ranged from 0.15 to 2 (green to orange) and evaporative index values from 0.13 to 0.9 (dark blue to green). The lowest energy and evaporative values were observed at the Pacific Ocean coast in Colombia and were associated to high cloud density over much of the year.

Figure 3.A shows the comparison of the long-term water-energy budget across climate classes in America through the Budyko curve. Results suggested that the water budget in tropical climates follows the Budyko theory (dots with black contour in Figure 3.A), meanwhile, the majority of extra tropical regions showed strong deviations with respect to the long-term water balance, where a higher radiation (AI) with respect to the evaporative ratio (EI) was observed.

At annual scales, energy and evaporative indexes (AI and EI) across tropical climates were relatively constant over the period 2000-2014 ( $\text{std}<0.15$  and  $\text{std}<0.06$ , respectively), such as shown in Figure 3.B and Figure 3.C. Nevertheless, more water-limited climates were subject to more abrupt changes in climatological conditions, e.g. savanna regions (As, light-green lines) exhibited an increase of  $\sim 100\%$  in dryness index (AI) from 2011 to 2012, associated to a decrease in precipitation from  $\sim 1,290$  to  $760$  mm/year likely due to El Niño conditions.



**Figure 2:** Mean annual Evaporative Index (a and c) and Dryness Index (b and d) across the tropics (18°S to 18°N) in America. c) and d) corresponds to que purple square in a) and b).



**Figure 3:** Water-energy budget across climates from the Köppen-Geiger classification explained by A) Budyko curve, B) annual variation of Dryness Index in tropical regions and C) annual variation of Evaporative Index in tropical regions. In the Budyko curve, tropical climates are displayed as dots with black contours.

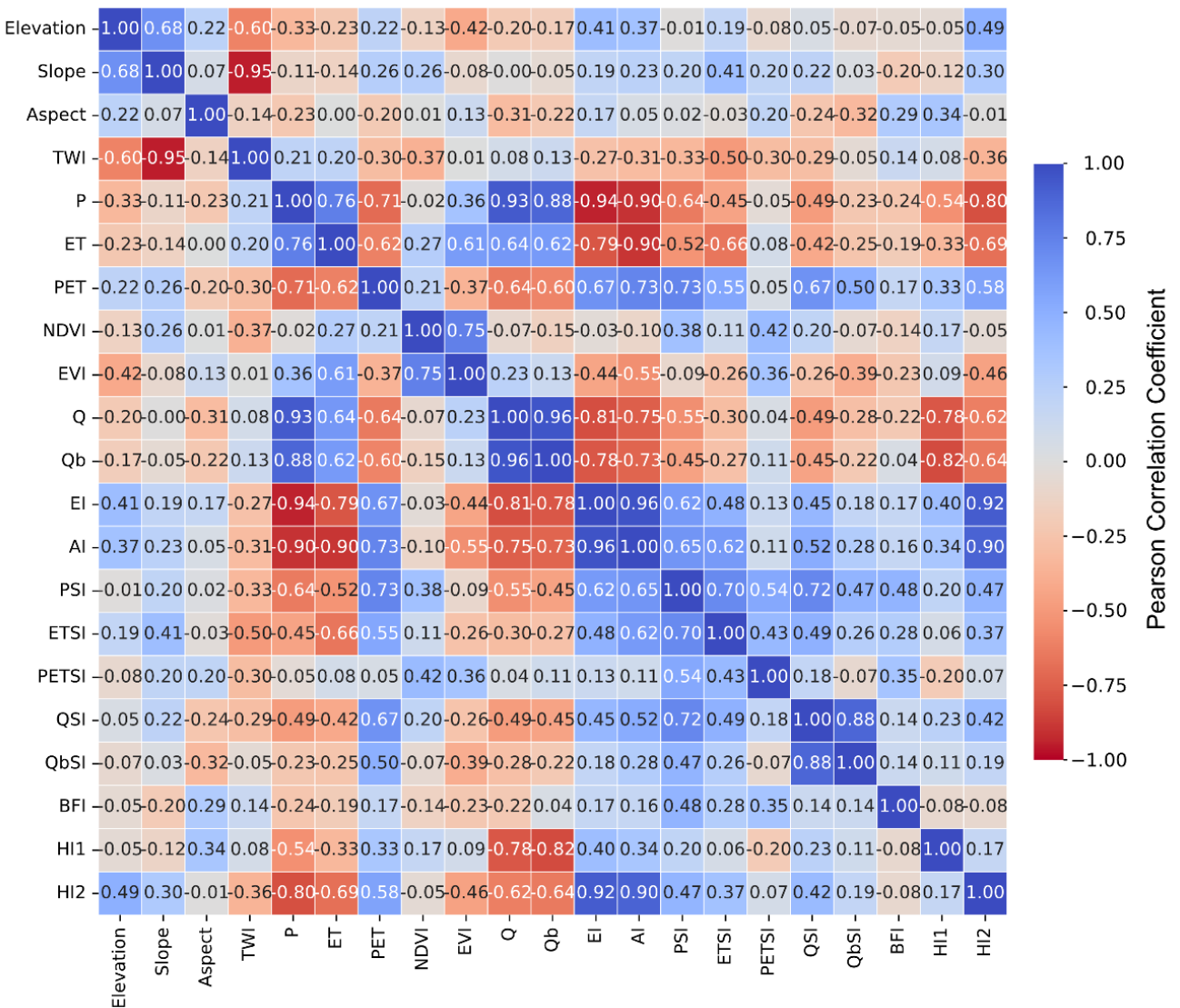
### 3.2 Catchment-scale eco-hydrological controls

Table 4 summarizes the catchments' eco-hydrological indicators for the common period from 2000 to 2014 associated to each catchment. Precipitation ranged from 930 to 4,700 mm/year with a median of 2,550 mm/year, with the wettest catchments being located in Costa Rica and the driest in Mexico. Actual evapotranspiration ranges from 900 to 1,350 mm/year and potential evapotranspiration from 1,580 to 2,080 mm/year. The dryness index (AI) varied from 0.35 to 2 and BFI ranged between 0.36 and 0.7. Mean annual streamflow reached 1,597 mm/year with a standard deviation of 850 mm/year, whereas, the Horton index averaged 0.50 with a standard deviation of 0.15.

**Table 4:** Mean annual climatology and eco-hydrology indicators for the study catchments. Q is the streamflow, BFI is the baseflow index, PSI is the seasonal precipitation index, HI1 and HI2 are the Horton Index derived from eq. (2) and (3).

Country	ID	P [mm/year]	AET [mm/year]	PET [mm/year]	EI	AI	Q [mm/year]	BFI	PSI	HI1	HI2
Mexico	1	1350.38	1077.09	1897.15	0.82	1.44	605.99	0.61	0.88	0.66	1.02
	2	1656.03	1165.79	2073.91	0.72	1.27	1368.72	0.56	1.01	0.25	1.16
	3	1527.82	958.62	2078.55	0.64	1.38	676.71	0.59	1.02	0.71	0.71
	4	2129.67	1215.87	1864.26	0.58	0.89	1133.33	0.54	0.88	0.63	0.77
	5	1973.55	1221.71	1900.64	0.63	0.98	1143.48	0.57	0.85	0.56	0.84
	6	930.52	901.63	1892.44	0.98	2.06	600.88	0.57	0.82	0.45	1.42
	7	1594.85	1143.95	1971.71	0.72	1.24	1042.9	0.61	0.75	0.45	0.99
	8	1879.04	1173.12	1892.76	0.63	1.02	991.19	0.58	0.85	0.6	0.83
Costa Rica	9	4703.67	1301.43	1658.57	0.28	0.36	4389.65	0.55	0.36	0.08	0.5
	10	3182.74	1296.3	1721.96	0.41	0.55	2113.72	0.54	0.57	0.46	0.62
	11	1997.66	1173.63	1793.07	0.6	0.92	940.81	0.68	0.68	0.64	0.65
	12	2552.99	1296.88	1612.66	0.52	0.64	1832.57	0.71	0.67	0.35	0.66
	13	2656.66	1351.83	1762.86	0.52	0.67	1246.21	0.52	0.63	0.67	0.71
	14	3074.25	1309.73	1692.49	0.43	0.56	2071.44	0.53	0.52	0.44	0.66
	15	3651.4	1295.44	1586.16	0.36	0.44	2889.84	0.37	0.28	0.46	0.64
	16	2710.49	1338.07	1833.56	0.5	0.68	1704.43	0.63	0.63	0.47	0.67
	17	3004.18	1325.87	1690.12	0.45	0.57	2743.54	0.57	0.54	0.21	0.65
	18	1761.2	1194.77	1894.84	0.7	1.11	786.02	0.61	0.82	0.66	0.85
Colombia	19	3346.82	1259.99	1759.92	0.38	0.53	2123.81	0.53	0.39	0.51	0.56
	20	3011.91	1243.27	1787.39	0.42	0.6	1848.43	0.59	0.4	0.5	0.57
	21	2007.72	1136.66	1615.74	0.57	0.82	1165.13	0.58	0.32	0.53	0.8
	22	3053.13	1299.9	1755.26	0.43	0.58	2482.04	0.51	0.36	0.31	0.71
	23	2844.18	1238.4	1800.73	0.44	0.63	1625.32	0.61	0.43	0.55	0.57
	24	3074.17	1253.19	1706.81	0.41	0.56	2132.49	0.57	0.37	0.42	0.6
	25	1517.83	1177.35	1858.89	0.79	1.24	786.68	0.4	0.34	0.7	1.13
	26	2135.67	1216.84	1852.2	0.57	0.87	1346.48	0.54	0.31	0.54	0.79
	27	2710.93	1280.66	1753.97	0.48	0.65	1327.35	0.45	0.29	0.67	0.73

The degree of dependence between the topographical, climatological and ecological indicators is shown as a correlation matrix in Figure 4. Topographic parameters were found to be more associated with climate and vegetation than streamflow generation. Mean elevation had a positive correlation with dryness and evaporative indexes (0.41 and 0.37, respectively) and with vegetation water use efficiency described by equation 3 (HI2) ( $p=0.49$ ). Slope was positively correlated to evapotranspiration seasonality (ETSI) and HI2 (0.41 and 0.3). Aspect was mainly correlated to the Horton index computed with equation 2 (HI1) and was negatively correlated with mean annual streamflow ( $p=-0.31$ ). Surprisingly, the topographic wetness index (TWI) was strongly negatively correlated ( $-0.5 < p < -0.3$ ) with several climate and vegetation attributes (NDVI, HI2, PSI, ETSI), but had little control on the spatial distribution of mean annual streamflow ( $p=0.08$ ).



**Figure 4:** Correlation matrix of the eco-hydrology indicators of the 27 catchments. P is precipitation; ET is actual evapotranspiration; PET is potential evapotranspiration; EI is evaporative index; AI is dryness index; Q is streamflow; Qb is baseflow; BFI is baseflow index; PSI, ETSI, PETSI, QSI and QbSI are the seasonal index of P, ET, PET, Q and Qb, respectively; HI1 and HI2 are the Horton index derived with equations 2 and 3.

Mean annual streamflow and baseflow were found to be mainly controlled by the amount of precipitation ( $p=0.93$  and  $0.88$ , respectively). Moreover, evaporative and dryness indexes were identified as second order factors, not surprising since tropical climates were found to agree with Budyko's theory. Furthermore, vegetation water use (HI1) exhibited a higher control on catchment responses (with correlations of  $Q=-0.78$  and  $Qb=-0.82$ , respectively) in comparison with climate drivers (e.g. AET, PET and seasonality).

On the other hand, vegetation water use efficiency (HI1 and HI2) was found negatively correlated to precipitation ( $p=-0.54$  and  $-0.8$ , respectively) and positively correlated to EI and AI. Indeed, the Horton index HI1 and HI2 seemed to be dependent on the data used to compute it. Therefore, HI1 presented higher a correlation to streamflow ( $p=-0.78$ ) and HI2 to evaporative index ( $p=0.92$ ). Nevertheless, HI1 and HI2 were poorly correlated ( $0.17$ ), maybe due to the higher uncertainty in AET estimates (used to computed HI2).

### 3.3 Water use efficiency across tropical catchments

The spatial variation of vegetation water use efficiency described by HI1 is shown in Figure 5. Variable patterns were not observed across latitude, but since HI1 was negatively correlated with precipitation (Figure 4), wetter catchments are less efficient in terms of vegetation water use. Such a lower water use efficiency is emphasized by the wet Costa Rican catchments exhibiting mean HI1 and HI2 of 0.44 and 0.66, respectively. Colombian catchments presented mean annual Horton indexes of 0.53 and 0.72, with the drier Mexican catchments showing the highest values of 0.54 and 0.97, respectively.

Selected annual temporal series in Figure 5 suggested that in spite of precipitation changes (blue line), contributions of subsurface reservoirs to total streamflow described by the BFI (red line) and vegetation growth described by NDVI (green line) remained relatively constant over time in several catchments (e.g. ID 1, 5, 17, 20, 26). Furthermore, Horton indexes (black continuous and dashed line) were not obviously correlated with vegetation growth and no pattern with respect to precipitation was observed. However, some catchments (ID 1, 8, 20) HI1 and HI2 increased during dry years since vegetation tends to be increasingly water efficient during droughts (Arciniega-Esparza et al., 2017; Troch et al., 2009). Nevertheless, other catchments (e.g. ID 15, 17, 20) showed an opposite behavior, where water efficiency increased with water availability. In some Mexican catchments (e.g. ID 1) we found unrealistic HI2 values higher than 1 due to input data uncertainty.

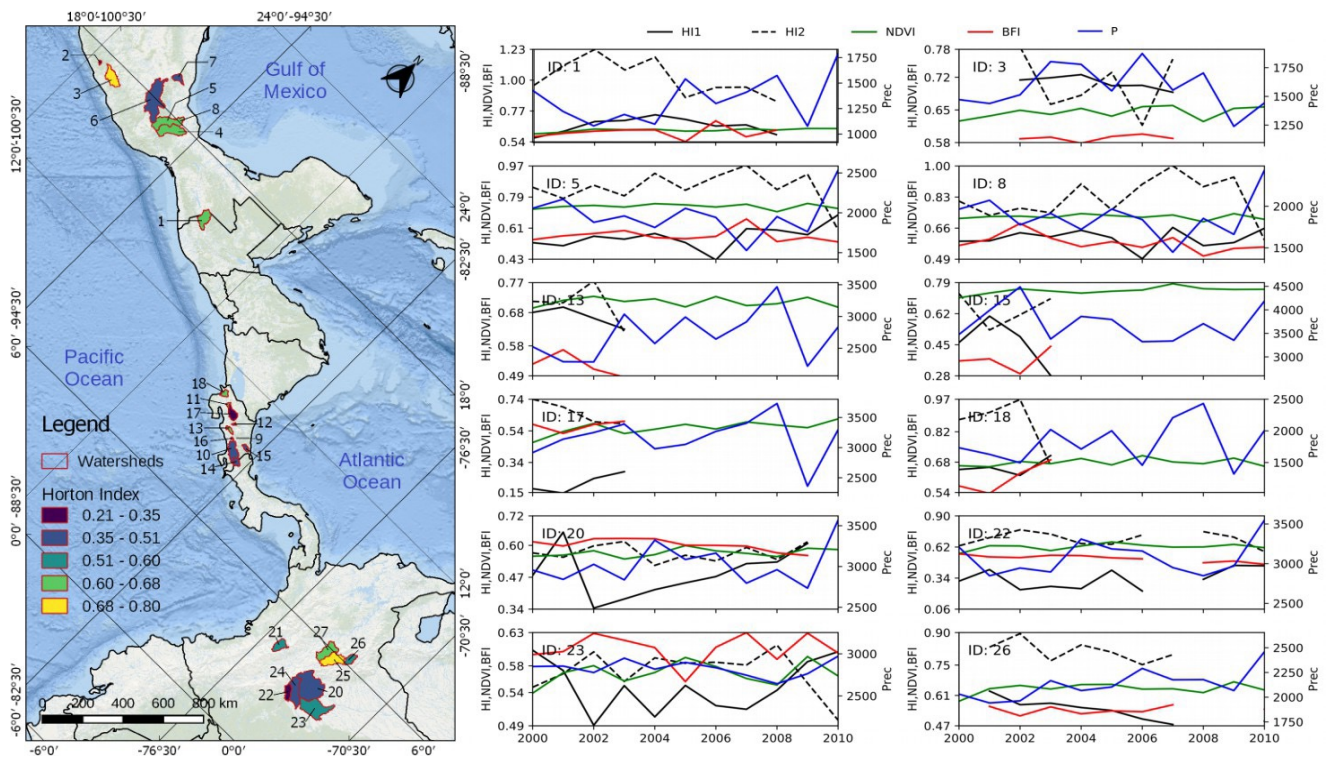


**Figure 5:** Spatial distribution of mean annual Horton Index and annual time series of HI, NDVI, BFI and precipitation. The HI1 and HI2 were computed with eq. (2) and eq. (3), respectively.

### 3.4 Streamflow eco-hydrological controls

Long-term and annual streamflow partitioning was analyzed in terms of climate and vegetation variation. Figure 6 suggested that long-term precipitation and Horton index grouped the shape of flow duration curves according to high water availability and lower vegetation water use reflected by higher flows over the interquartile range (frequency 0.25-0.75). To the contrary, higher water efficiency of terrestrial vegetation and lower amounts of precipitation tended to reduce the proportion of low flows.

At annual scales, streamflow for the 27 catchments was strongly controlled by the dryness index following a non-linear regression model ( $r^2=0.83$ ,  $p<0.05$ ) and to a second order by a lineal dependency with the Horton index ( $r^2=0.53$ ,  $p<0.05$ ) as shown in Figure 7. Also, note that the fitted equation using AI as predictor showed a remarkable similarity with Budyko's theory, where  $Q/P=AET/P-1$ . Therefore, the water-energy balance was preserved not only at long-term time scales but also on an annual scale. Vegetation control on streamflow was unclear for some wetter and the most arid catchments (ID 9, in Costa Rica and ID 6, in Mexico). Here, the scatter plot showed those catchments as outliers, and the AI model located catchments 6 and 9 on the boundaries.

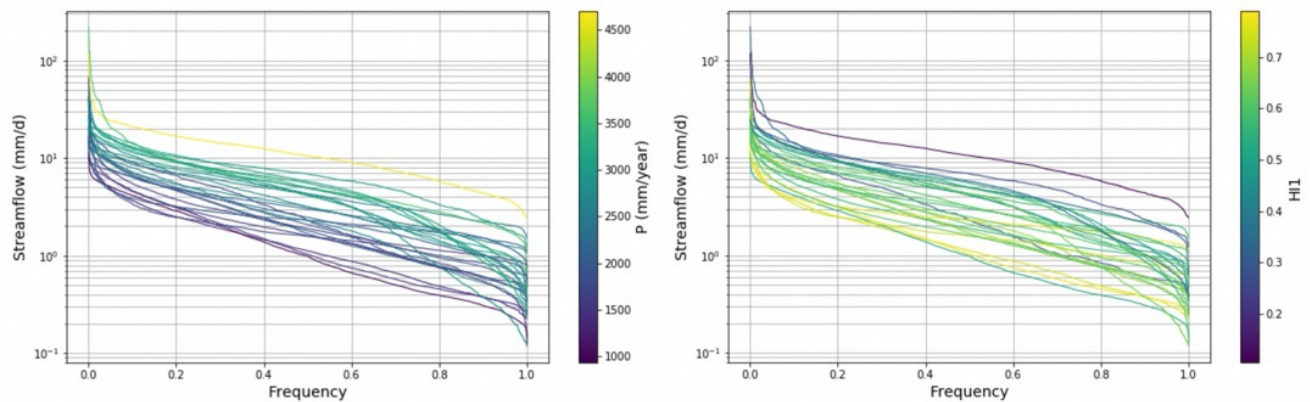


**Figure 6:** Streamflow duration curve variation explained by mean annual precipitation (left) and mean Horton index computed with equation 2 (right).

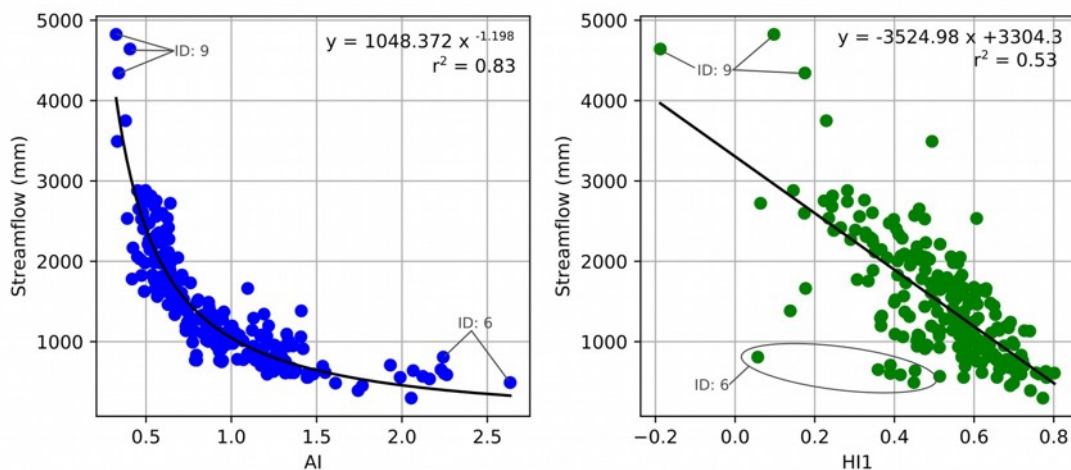


**Figure 7:** Annual streamflow explained by dryness index (left) and Horton index (right).

---

## 4. Discussion

### 4.1 Catchment-scale eco-hydrological patterns

Despite the complexity of soil-vegetation-climate interactions, long-term hydroclimatic conditions in tropical climates in America were well described by the Budyko curve (Figure 3), in comparison with extra-tropical climates that deviated with respect to the theory. Therefore, the Budyko theory may be used in tropical catchments to explore streamflow elasticity and catchment resilience to climate change (Esquivel-Hernández et al., 2017; Koppa et al., 2021; Peña-Arancibia et al., 2012; Renner and Bernhofer, 2012). Although precipitation is typically most strongly correlated with flow generation, a European regional study suggests that intra-annual variation in precipitation and increased PET due to rising temperatures from climate change may significantly impact streamflow (Collignan et al., 2023).

We also found that climate was the main driver of long-term water partitioning in line with previous work by e.g. Gan et al. (2021), Collignan et al. (2023), and Zanardo et al. (2012). Mean annual precipitation exhibited the strongest linear control on the mean annual streamflow and baseflow (see correlation matrix in Figure 4). Furthermore, the dryness index (ratio of potential evapotranspiration and precipitation) improved such predictions through a non-linear relationship (Figure 7). Similar results were reported identifying the dryness index as a key indicator to classify annual and intra-annual hydrological catchment response over large climate gradients (Kuentz et al., 2017; Trancoso et al., 2016; Zhang et al., 2018).

Recent studies have linked the water-energy balance theory to vegetation indicators (Chen et al., 2023; Luo et al., 2020), such as the water use, rooting depth, and fractional vegetation cover to further improve ecohydrological understanding (Chen et al., 2023; Donohue et al., 2012; Gan et al., 2021; Zhang et al., 2001).

However, vegetation rooting depths was observed to be shorter in regions with less precipitation seasonality and generally higher water availability (Gao et al., 2014). The tropical catchments presented a largely uniform climatology as opposed to extra-tropics and the Budyko theory pointed at vegetation that is less important for water partitioning. However, Budyko does not directly consider the partitioning into evaporation and transpiration, with the latter being likely the more important water flux and directly linked to the vegetation (Schlesinger & Jasechko, 2014). Tropical biomes showed an important role on water partitioning taking transpiration directly into account (Good et al., 2017).

Nonetheless, the vegetation dynamics were consistent with previous studies, where vegetation water use was found to contain information about climate and landscape interactions (Troch et al., 2009; Voepel et al., 2011). Furthermore, vegetation water use showed higher negative correlations with baseflow than streamflow ( $\rho=-0.82$  and  $-0.78$ , respectively). Such behavior can be explained since vegetation evolves to be more water efficient (deeper roots and higher water retention capacity) in dry environments and under water stress playing a more important role on the partitioning of flow generation and groundwater recharge (Arciniega-Esparza et al., 2017; Gao et al., 2014).

### 4.2 Can we learn about eco-hydrological processes from remote sensing?

The lack of in-situ data is one of the significant limitations in long-term water balance assessments and in understanding hydrological processes. Hydrometric data for Mexico and Colombia were filtered to consider good-quality data with natural flow patterns, significantly limiting the number of stations available in tropical climate zones. On the other hand, data from Costa Rica are not publicly available, and only ICE data is available. This

---

was reflected in a short standard period between hydrometric data and remote sensing climatological data, affecting the long-term balance synthesis. Other hydrometric data in Central American countries were discarded due to the lack of quality of information.

Sheffield et al. (2018) gives a good overview of remote sensing and global products for use in hydrology studies of data scarce areas such as Latin America. Here, we already use some of the mentioned products in our eco-hydrological assessment, which could be expanded towards including soil moisture data and remotely sensed water levels.

However, all remote sensors require calibration using station data and we found issues in this regard using actual evapotranspiration from MODIS16, where HI2 values higher than 1 were observed indicating that ET is higher than P-Q in some Mexican catchments. Overestimation of MODIS ET products was also reported from other regions around the world (Liu et al., 2015; Mu et al., 2007, 2011b), mainly associated to the complexity of the vegetation dynamics and the lack of station data for the algorithm calibration (Raoufi & Beighley, 2017). Previous studies have highlighted that evapotranspiration, mainly derived from remote sensing and global products, is one of the significant sources of uncertainty in water balances, increasing discrepancies with Budyko's results (Koppa et al., 2021; Xiong et al., 2023).

Since we consider ET as our most uncertain variable compared to rainfall (CHIRPS undergoes a calibration procedure) and measured streamflow, the Horton Index estimated with equation 2 (HI1) was preferred for our interpretation of results.

Monthly precipitation from TRMM was widely used in the global tropics with good correlation compared to ground gauges (Erazo et al., 2018; Senent-Aparicio et al., 2018), but coarse spatial resolution of TRMM is a limitation for its application in Central America due to the relatively small size of some catchments (<900 km<sup>2</sup>). Therefore, the CHIRPS product with a higher spatial resolution seems to be a better option in complex topography with microclimates (Ullah et al., 2019; Zambrano-Bigiarini et al., 2017).

We found that the dryness index derived from MODIS and CHIRPS is able to explain the annual catchment response (Figure 7,  $r^2=0.83$ ). The fitted equation might be useful as a first-order estimation for water management since it can be directly used to predict annual streamflow in ungauged catchments and allows to evaluate effects of climate change on the water balance.

---

## 5. Conclusion

Eco-hydrological patterns were analyzed in 27 tropical catchments across Colombia, Costa Rica and Mexico for the period 2000-2014 using measured streamflow records, remote sensing and merged databases for precipitation, evapotranspiration and vegetation dynamics. Most of the Colombian and Costa Rican catchments were classified as energy-limited ( $AI < 1$ ), whereas, Mexican catchments tended to be water-limited ( $AI > 1$ ).

Furthermore, tropical climates were observed to follow the theoretical water-energy curve described by Budyko, in comparison to most of the extra-tropical regions that presented high values of the dryness index ( $AI$ ) with respect to their evaporative index ( $EI$ ).

Vegetation water use efficiency in the study catchments was analyzed through the Horton Index ( $HI$ ), computed using the equation proposed by Troch et al. (2009), where vaporization ( $V$ ) was considered as  $P-Q$  and as  $AET$  from MODIS16. We found poor correlation between both  $HI$  indexes ( $\rho = 0.17$ ). The MODIS ET accuracy was not the purpose of this research, but the ET overestimation could be associated to the lack of ground data used to calibrate the parameters of the ET algorithm in tropical biomes.

Results suggested that water use efficiency is linearly correlated with streamflow and baseflow, even at annual scales. Furthermore, the dryness index was found as the most important driver of catchment response. Such findings support the importance of climate and vegetation on hydrologic partitioning and how ecosystems evolve to be more water efficient under water stress and climate change.

Finally, global products and in-situ measurements improved the understanding of ecohydrological processes at catchment scales particularly in the data scarce tropical region of Latin America. Future work will focus on better calibration and subsequently bias-adjustments of global products using local station networks for use at higher temporal and spatial scales. Together with more widespread availability of field measurements allowing water partitioning of evapotranspiration into evaporation and transpiration, finer scale global products have the potential to revolutionize large-scale eco-hydrology particularly in the tropics.

---

## 6. Acknowledgments

Saúl Arciniega-Esparza was supported by the SECIHTI' SNI (National System of Researchers of the Secretariat of Science, Humanities, Technology and Innovation) program from Mexico. Christian Birkel wants to thank UCREA, TropiSeca and the Water and Global Observatory for support to work on this paper.

---

## 7. References

- Arciniega-Esparza, S., Breña-Naranjo, J.A., & Troch, P.A. (2017). On the connection between terrestrial and riparian vegetation: the role of storage partitioning in water-limited catchments. *Hydrological Processes*, 31 (2), 489–494. DOI: 10.1002/hyp.11071
- Beck, H.E., de Roo, A., & van Dijk, A.I.J.M. (2015). Global Maps of Streamflow Characteristics Based on Observations from Several Thousand Catchments. *Journal of Hydrometeorology* 16 (4): 1478–1501. DOI: 10.1175/JHM-D-14-0155.1
- Birkel, C., Soulsby, C., & Tetzlaff, D. (2012). Modelling the impacts of land-cover change on streamflow dynamics of a tropical rainforest headwater catchment. *Hydrological Sciences Journal*, 57(8), 1543–1561. <https://doi.org/10.1080/02626667.2012.728707>
- Brooks, P.D., Troch, P.A., Durcik, M., Gallo, E.L., Moravec, B.G.E. MS, & Carlson, M. (2011). Quantifying regional-scale ecosystem response to changes in precipitation: Not all rain is created equal. *Water Resour. Res.*, 47 (W00J08) DOI: 10.1029/2010WR009762
- Bruijnzeel, L.A. (2004). Hydrological functions of tropical forests: Not seeing the soil for the trees?. *Agriculture, Ecosystems & Environment*, 104 (1), 185-228. DOI: 10.1016/j.agee.2004.01.015
- Budyko, M.I. (1974). *Climate and life*. Int. Geophys. Ser. 1st Edition, Volume 18. ISBN: 9780080954530
- Chen, Y., Chen, X., Xue, M., Yang, C., Zheng, W., Cao, J., Yan, W., & Yuan, W. (2023). Revisiting the hydrological basis of the Budyko framework with the principle of hydrologically similar groups. *Hydrology and Earth System Sciences*, 27(9), 1929–1943. <https://doi.org/10.5194/hess-27-1929-2023>
- Collignan, J., Polcher, J., Bastin, S., & Quintana-Segui, P. (2023). Budyko Framework Based Analysis of the Effect of Climate Change on Watershed Evaporation Efficiency and Its Impact on Discharge Over Europe. *Water Resources Research*, 59(10). <https://doi.org/10.1029/2023WR034509>
- Conrad, O., Bechtel, B., Bock, M., Dietrich, H., Fischer, E., Gerlitz, L., Wehberg, J., Wichmann, V., & Böhner, J. (2015). System for Automated Geoscientific Analyses (SAGA) v. 2.1.4. *Geoscientific Model Development*, 8, 1991–2007. DOI: 10.5194/gmd-8-1991-2015
- Didan, K. (2015). MOD13Q1 - MODIS/Terra Vegetation Indices 16-Day L3 Global 250m SIN Grid. [Dataset] NASA EOSDIS Land Processes Distributed Active Archive Center. DOI: 10.5067/MODIS/MOD13Q1.006
- Donohue, R.J., Roderick, M.L., & McVicar, T.R. (2012). Roots, storms and soil pores: Incorporating key ecohydrological processes into Budyko's hydrological model. *Journal of Hydrology*, 436–437 (0): 35–50. DOI: 10.1016/j.jhydrol.2012.02.033
- Erazo, B., Bourrel, L., Frappart, F., Chimborazo, O., Labat, D., Dominguez-Granda, L., Matamoros, D., & Mejia, R. (2018). Validation of satellite estimates (Tropical Rainfall Measuring Mission, TRMM) for rainfall variability over the Pacific slope and Coast of Ecuador. *Water*, 10 (2). DOI: 10.3390/w10020213
- Esquivel-Hernández, G., Sánchez-Murillo, R., Birkel, C., Good, S.P., & Boll, J. (2017). Hydroclimatic and ecohydrological resistance/resilience conditions across tropical biomes of Costa Rica. *Ecohydrology* 10 (6): 1–12. DOI: 10.1002/eco.1860
- Farr, T.G., Rosen, P.A., Caro, E., Crippen, R., Duren, R., Hensley, S., Kobrick, M., Paller M., Rodriguez, E., Roth, L., Seal, D., Shaffer, S., Shimada, J., Umland, J., Werner, M., Oskin, M., Burbank, D., & Alsdorf, D. (2007). The shuttle radar topography mission. *Reviews of Geophysics*, 45. DOI: 10.1029/2005RG000183
- Funk, C., Verdin, A., Michaelsen, J., Peterson, P., Pedreros, D., & Husak, G. (2015). A global satellite-assisted precipitation climatology. *Earth Syst. Sci. Data*, 7: 275–287. DOI: 10.5194/essd-7-275-2015
- Gan, G., Liu, Y., & Sun, G. (2021). Understanding interactions among climate, water, and vegetation with the Budyko framework. In *Earth-Science Reviews* (Vol. 212). Elsevier B.V. <https://doi.org/10.1016/j.earscirev.2020.103451>
- Gao, H., Hrachowitz, M., Schymanski, S.J., Fenicia, F., Sriwongsitanon, N., & Savenije, H.H.G. (2014). Climate controls how ecosystems size the root zone storage capacity at catchment scale. *Geophysical Research Letters*, 41 (22): 7916–7923. DOI: 10.1002/2014GL061668
- Gnann, S., Baldwin, J. W., Cuthbert, M. O., Gleeson, T., Schwanghart, W., & Wagener, T. (2025). The Influence of Topography on the Global Terrestrial Water Cycle. *Reviews of Geophysics*, 63(1). <https://doi.org/10.1029/2023RG000810>
- Good, S.P., Moore, G.W., & Miralles, D.G. (2017). A mesic maximum in biological water use demarcates biome sensitivity to aridity shifts. *Nature Ecology and Evolution* 1 (12): 1883–1888 DOI: 10.1038/s41559-017-0371-8 Horton RE. 1933. The

- role of infiltration in hydrologic cycle. *Trans. Am. Geophys. Union* 14: 446–460
- Guswa, A. J., Tetzlaff, D., Selker, J. S., Carlyle-Moses, D. E., Boyer, E. W., Bruen, M., Cayuela, C., Creed, I. F., van de Giesen, N., Grasso, D., Hannah, D. M., Hudson, J. E., Hudson, S. A., Iida, S., Jackson, R. B., Katul, G. G., Kumagai, T., Llorens, P., Lopes Ribeiro, F., ... Levia, D. F. (2020). Advancing ecohydrology in the 21st century: A convergence of opportunities. In *Ecohydrology* (Vol. 13, Issue 4). John Wiley and Sons Ltd. <https://doi.org/10.1002/eco.2208>
- Huxman, T.E., Smith, M.D., Fay, P.A., Knapp, A.K., Shaw, M.R., Lolk, M.E., Smith, S.D., Tissue, D.T., Zak, J.C., Weltzin, J.F., et al. (2004). Convergence across biomes to a common rain-use efficiency. *Nature*, 429 (6992): 651–654. DOI: 10.1038/nature02561
- Koppa, A., Alam, S., Miralles, D. G., & Gebremichael, M. (2021). Budyko-Based Long-Term Water and Energy Balance Closure in Global Watersheds From Earth Observations. *Water Resources Research*, 57(5). <https://doi.org/10.1029/2020WR028658>
- Krishnaswamy, J., Kelkar, N., & Birkel, C. (2018). Positive and neutral effects of forest cover on dry-season stream flow in Costa Rica identified from Bayesian regression models with informative prior distributions. *Hydrological Processes*, 32 (24): 3604–3614 DOI: 10.1002/hyp.13288
- Kuentz, A., Arheimer, B., Hundecha, Y., & Wagener, T. (2017). Understanding hydrologic variability across Europe through catchment classification. *Hydrol. Earth Syst. Sci.*, 21: 2863–2879. DOI: 10.5194/hess-21-2863-2017
- Liu, Z., Shao, Q., & Liu, J. (2015). The performances of MODIS-GPP and -ET products in China and their sensitivity to input data (FPAR/LAI). *Remote Sensing*, 7 (1): 135–152. DOI: 10.3390/rs70100135
- Luo, Y., Yang, Y., Yang, D., & Zhang, S. (2020). Quantifying the impact of vegetation changes on global terrestrial runoff using the Budyko framework. *Journal of Hydrology*, 590. <https://doi.org/10.1016/j.jhydrol.2020.125389>
- Lyne, V., & Hollick, M. (1979). Stochastic time variable rainfall runoff modeling. National Committee on Hydrology and Water Resources of the Institution of Engineers (Hydrology and Water Resources Symposium Perth 1979 Proceedings): 89–92.
- Montanari, L., Sivapalan, M., & Montanari, A. (2006). Investigation of dominant hydrological processes in a tropical catchment in a monsoonal climate via the downward approach. *Hydrology and Earth System Sciences*, 10 (5): 769–782. DOI: 10.5194/hess-10-769-2006
- Moore, G., McGuire, K., Troch, P., & Barron-Gafford, G. (2015). Ecohydrology and the Critical Zone: Processes and Patterns Across Scales. In *Developments in Earth Surface Processes* (Vol. 19, pp. 239–266). Elsevier. <https://doi.org/10.1016/B978-0-444-63369-9.00008-2>
- Mu, Q., Heinsch, F.A., Zhao, M., & Running, S.W. (2007). Development of a global evapotranspiration algorithm based on MODIS and global meteorology data. *Remote Sensing of Environment*, 106 (3): 285–304. DOI: 10.1016/j.rse.2006.07.007
- Mu, Q., Zhao, M., & Running, S.W. (2011). Improvements to a MODIS global terrestrial evapotranspiration algorithm. *Remote Sensing of Environment*, 115 (8): 1781–1800. DOI: 10.1016/j.rse.2011.02.019
- Muñoz-Jiménez, R., Giraldo-Osorio, J.D., Brenes-Torres, A., Avendaño-Flores, I., Nauditt, A., Hidalgo-León, H.G., & Birkel, C. (2018). Spatial and temporal patterns, trends and teleconnection of cumulative rainfall deficits across Central America. *International Journal of Climatology*, (November): 1–14 DOI: 10.1002/joc.5925
- Nemani, R.R., Keeling, C.D., Hashimoto, H., Jolly, W.M., Piper, S.C., Tucker, C.J., Myneni, R.B., Running, S.W. (2003). Climate-driven increases in global terrestrial net primary production from 1982 to 1999. *Science*, 300, 1560–1563. DOI: 10.1126/science.1082750
- Peel, M.C., B. L. F., & McMahon, T.A. (2007). Updated world map of Köppen-Geiger climate classification. *Hydrol. Earth Syst. Sci.*, 11: 1633–1644. DOI: 10.5194/hess-11-1633-2007
- Peña-Arancibia, J.L., van Dijk, A.I.J.M., Guerschman, J.P., & Mulligan, M. (Sampurno) Bruijnzeel, L.A., & McVicar, T.R. (2012). Detecting changes in streamflow after partial woodland clearing in two large catchments in the seasonal tropics. *Journal of Hydrology*, 416–417, 60–71. DOI: 10.1016/j.jhydrol.2011.11.036
- Peña-Arancibia, J.L., van Dijk, A.I.J.M., Mulligan, M., & Bruijnzeel, L.A. (2010). The role of climatic and terrain attributes in estimating baseflow recession in tropical catchments. *Hydrology and Earth System Sciences*, 14: 2193–2205. DOI: 10.5194/hess-14-2193-2010
- Pokhrel, Y.N., Fan, Y., Miguez-Macho, G., Yeh, P.J.F., & Han, S.C. (2013). The role of groundwater in the Amazon water cycle: 3. Influence on terrestrial water storage computations and comparison with GRACE. *Journal of Geophysical Research Atmospheres*, 118 (8): 3233–3244. DOI: 10.1002/jgrd.50335

- Prentice, I.C., Farquhar, G.D., Fasham, M.J.R., Goulden, M.L., Heimann, M., Jaramillo, V.J., Kheshgi, H.S., Quéré, C. Le., QuScholes, R.J., & Wallace, D.W. (2001). The carbon cycle and atmospheric carbon dioxide. In *Climate Change 2001: The Scientific Basis. Contribution of Working Group I to the Third Assessment Report of the Intergovernmental Panel on Climate Change* 183–237. DOI: 10.1097/MPG.0000000000001744
- Raoufi, R., & Beighley, E. (2017). Estimating daily global evapotranspiration using penman-monteith equation and remotely sensed land surface temperature. *Remote Sensing*, 9 (11) DOI: 10.3390/rs9111138
- Renner, M., & Bernhofer, C. (2012). Applying simple water-energy balance frameworks to predict the climate sensitivity of streamflow over the continental United States. *Hydrology and Earth System Sciences*, 16 (8): 2531–2546 DOI: 10.5194/hess-16-2531-2012
- Sawicz, K., Wagener, T., Sivapalan, M., Troch, P.A., & Carrillo, G. (2011). Catchment classification: Empirical analysis of hydrologic similarity based on catchment function in the eastern USA. *Hydrology and Earth System Sciences*, 15 (9): 2895–2911 DOI: 10.5194/hess-15-2895-2011
- Schlesinger, W.H., & Jasechko, S. (2014). Transpiration in the global water cycle. *Agricultural and Forest Meteorology*, 115-117. DOI: 10.1016/j.agrformet.2014.01.011
- Senent-Aparicio, J., López-Ballesteros, A., Pérez-Sánchez, J., Segura-Méndez, F.J., & Pulido-Velazquez, D. (2018). Using Multiple Monthly Water Balance Models to Evaluate Gridded Precipitation Products over Peninsular Spain. *Remote Sensing*, 10 (6): 922. DOI: 10.3390/rs10060922
- Sheffield, J., Wood, E.F., Pan, M., Beck, H., Coccia, G., Serrat-Capdevila, A., & Verbist, K. (2018). Satellite Remote Sensing for Water Resources Management: Potential for Supporting Sustainable Development in Data-Poor Regions. *Water Resources Research*, 54 (12): 9724–9758. DOI: 10.1029/2017wr022437
- Smakhtin, V.U. (2001). Low flow hydrology: A review. *Journal of Hydrology*, 240: 147–186. DOI: 10.1016/S0022-1694(00)00340-1
- Syvitski, J.P.M., Cohen, S., Kettner, A.J., & Brakenridge, G.R. (2014). How important and different are tropical rivers? - An overview. *Geomorphology*, 227: 5–17. DOI: 10.1016/j.geomorph.2014.02.029
- Thompson, S.E., Harman, C.J., Troch, P.A., Brooks, P.D., & Sivapalan, M. (2011). Spatial scale dependence of ecohydrologically mediated water balance partitioning: A synthesis framework for catchment ecohydrology. *Water Resources Research*, 47 (5): 1–20. DOI: 10.1029/2010WR009998
- Trancoso, R., Larsen, J.R., McAlpine, C., McVicar, T.R., & Phinn, S. (2016). Linking the Budyko framework and the Dunne diagram. *Journal of Hydrology*, 535 (February): 581–597. DOI: 10.1016/j.jhydrol.2016.02.017
- Troch, P. A., Carrillo, G.A., Heidbüchel, I., Rajagopal, S., Switanek, M., Volkmann, T.H.M., & Yaeger, M. (2009a). Dealing with landscape heterogeneity in watershed hydrology: A review of recent progress toward new hydrological theory. *Geography Compass*, 3: 375–392. DOI: 10.1111/j.1749-8198.2008.00186.x
- Troch, P.A., Martinez, G.F., Pauwels, V.R.N., Durcik, M., Sivapalan, M., Harman, C., Brooks, P.D., Gupta, H., & Huxman, T. (2009b). Climate and vegetation water use efficiency at catchment scales. *Hydrological Processes*, 23: 2409–496, 2414. DOI: 10.1002/hyp.7358
- Ullah, W., Wang, G., Ali, G., Fiifi, D., Hagan, T., Bhatti, A.S., & Lou, D. (2019). Comparing Multiple Precipitation Products against In-Situ Observations over Different Climate Regions of Pakistan. *Remote Sensing*, 11 (Observations, Modeling, and Impacts of Climate Extremes): 628. DOI: 10.3390/rs11060628
- Voepel, H., Ruddell, B., Schumer, R., Troch, P.A., Brooks, P.D., Neal, A., Durcik, M., & Sivapalan, M. (2011). Quantifying the role of climate and landscape characteristics on hydrologic partitioning and vegetation response. *Water Resources Research*, 47 (8): 1–13. DOI: 10.1029/2010WR009944
- Wagener, T., Sivapalan, M., Troch, P., & Woods, R. (2007). Catchment Classification and Hydrologic Similarity. *Geography Compass*, 1: 1–31. DOI: 10.1111/j.1749-8198.2007.00039.x
- Walsh, R.P.D., & Lawler, D.M. (1981). Rainfall seasonality spatial patterns and change through time. *Weather*, 36: 201–506208. DOI: 10.1002/j.1477-8696.1981.tb05400.x
- Xiong, J., Abhishek, Xu, L., Chandanpurkar, H. A., Famiglietti, J. S., Zhang, C., Ghiggi, G., Guo, S., Pan, Y., & Vishwakarma, B. D. (2023). ET-WB: water-balance-based estimations of terrestrial evaporation over global land and major global basins. *Earth System Science Data*, 15(10), 4571–4597. <https://doi.org/10.5194/essd-15-4571-2023>
- Yang, Y., Donohue, R.J., McVicar, T.R., & Roderick, M.L. (2015). An analytical model for relating global terrestrial carbon assimilation with climate and surface conditions using a rate limitation framework. *Geophysical Research Letters*, DOI:

10.1002/2015GL066835

- Yang Y, Donohue RJ, McVicar TR, Roderick ML, Beck HE. 2016. Long-term CO<sub>2</sub> fertilization increases vegetation productivity and has little effect on hydrological partitioning in tropical rainforest. *Journal of Geophysical Research: Biogeosciences*, 121 (1): 2125–2140 DOI: 10.1002/2016JG003475
- Zambrano-Bigiarini, M., Nauditt, A., Birkel, C., Verbist, K., & Ribbe, L. (2017). Temporal and spatial evaluation of satellite-based rainfall estimates across the complex topographical and climatic gradients of Chile. *Hydrology and Earth System Sciences*, 21 (2): 1295–1320 DOI: 10.5194/hess-21-1295-2017
- Zanardo, S., Harman, C.J., Troch, P.A., Rao, P.S.C., & Sivapalan, M. (2012). Intra-annual rainfall variability control on interannual variability of catchment water balance: A stochastic analysis. *Water Resources Research*, 48 (1) DOI: 10.1029/2010WR009869
- Zhang, D., Liu, X., & Bai, P. (2018). Different influences of vegetation greening on regional water-energy balance under different climatic conditions. *Forests*, 9 (7): 1–15 DOI: 10.3390/f9070412
- Zhang, L., Dawes, W.R., & Walker, G.R. (2001). Response of mean annual evapotranspiration to vegetation changes at catchment scale. *Water Resources Research*, 37: 701–708 DOI: 10.1016/0950-4214(90)80029-K
- Zhang, M., Liu, N., Harper, R., Li, Q., Liu, K., Wei, X., Ning, D., Hou, Y., & Liu, S. (2017). A global review on hydrological responses to forest change across multiple spatial scales: Importance of scale, climate, forest type and hydrological regime. *Journal of Hydrology*, 546: 44–59 DOI: 10.1016/j.jhydrol.2016.12.040.
- Zomer, R. J., Xu, J., & Trabucco, A. (2022). Version 3 of the Global Aridity Index and Potential Evapotranspiration Database. *Scientific Data*, 9(1). <https://doi.org/10.1038/s41597-022-01493-1>
-